Published in final edited form as:
J Org Chem. 2012 January 6; 77(1): 5–16. doi:10.1021/jo201845z.

C2′-Pyrene-functionalized Triazole-linked DNA: Universal DNA/RNA Hybridization Probes

Sujay P. Sau and **Patrick J. Hrdlicka***
Department of Chemistry, University of Idaho, Moscow, ID-83844, USA

Abstract

Development of universal hybridization probes, i.e., oligonucleotides displaying identical affinity toward matched and mismatched DNA/RNA targets, has been a longstanding goal due to potential applications as degenerate PCR primers and microarray probes. The classic approach toward this end has been the use of ‘universal bases’ that either are based on aromatic base analogs without hydrogen-bonding capabilities or hydrogen-bonding purine derivatives. However, development of probes that enable truly ‘universal’ hybridization without compromising duplex thermostability has proven challenging. Here we have used the ‘click reaction’ to synthesize four C2′-pyrene-functionalized triazole-linked 2′-deoxyuridine phosphoramidites. We demonstrate that oligodeoxyribonucleotides modified with the corresponding monomers display: a) minimally decreased thermal affinity toward DNA/RNA complements relative to reference strands; b) highly robust universal hybridization characteristics (average differences in thermal denaturation temperatures of matched vs mismatched duplexes are < 1.5 °C); and c) exceptional affinity toward DNA targets containing abasic sites opposite of the modification site (ΔT_m up to +25 °C). The latter observation, along with results from absorption and fluorescence spectroscopy, indicates that the pyrene moiety is intercalating into the duplex whereby the opposing nucleotide is pushed into an extrahelical position. These properties render C2′-pyrene-functionalized triazole-linked DNA as promising universal hybridization probes for applications in nucleic acid chemistry and biotechnology.

1. INTRODUCTION

The Cu^I catalyzed [3+2] azide-alkyne cycloaddition (CuAAC) reaction, which results in the formation of 1,4-disubstituted 1,2,3-triazoles,[1,2] has been extensively utilized for the synthesis of modified nucleosides, nucleotides and oligonucleotides.[3,4] The remarkable progress over the past five years has paved the way for empowering applications in nucleic acid chemistry[5] such as post-synthetic labeling of oligonucleotides with reporter groups,[6] controlled metallization of oligonucleotides,[7] ligation of oligonucleotides,[8,9] and generation of oligonucleotides with artificial backbone[10] and nucleobase[11,12] motifs.

Our interest in a) employing the CuAAC reaction within oligonucleotide chemistry;[13] b) studying pyrene-functionalized oligonucleotide probes for potential diagnostic applications;[13–17] and c) developing oligonucleotides modified with 2′-intercalator-functionalized nucleotide monomers for DNA-targeting applications,[18–21] prompted us to explore oligodeoxyribonucleotides (ONs) that are modified with C2′-pyrene-functionalized triazole-linked 2′-deoxyuridine monomers **W**-**Z** (Figure 1). We surmised that the corresponding phosphoramidites would be readily available via CuAAC reactions using simple reagents and starting materials, and that the pyrene moiety of monomers **W**-**Z**

hrdlicka@uidaho.edu.

intercalates into duplex cores as observed with O2′-intercalator-functionalized RNA[21–23], N2′-intercalator-functionalized 2′-*N*-methyl-2′-amino-DNA,[21,24] and N2′-intercalator-functionalized 2′-amino-α-L-LNA monomers.[18–20] Moreover, monomers **W**-**Z** were selected to study the influence of the linker between the pyrene and triazole moieties on hybridization properties of correspondingly modified ONs, while non-functionalized monomer **V** provides insight into the relative roles of pyrene and triazole moieties. Recent reports have described pre- [25,26] and post-synthetic[6e,27] uses of the CuAAC reaction for 2′-functionalization of nucleotides. However, the present work is the first example of ONs modified with monomers where pyrene-functionalized 1,2,3-triazolyl moieties are directly attached to the 2′-position of nucleosides.

Here we demonstrate that ONs modified with C2′-pyrene-functionalized triazole-linked monomers are robust universal DNA/RNA hybridization probes, i.e., they display virtually identical DNA/RNA target affinity regardless of the nucleotide opposite of the modification site. Development of universal hybridization probes has been a longstanding goal due to their potential as degenerate PCR primers and microarray probes when the identity of one or more nucleotides in a target sequence is unknown.[28–31] The classic approach toward this end has been the use of ONs containing ‘universal bases’,[32] which fall into two categories: a) aromatic base analogs without hydrogen-bonding capabilities such as 3-nitropyrrole,[29] 5-nitroindole,[33] isocarbostyril[34] or pyrene,[13,35–38] and b) hydrogen-bonding universal bases based on inosine[39–41] or other purine moieties.[42,43] However, development of truly ‘universal’ hybridization probes that do not compromise duplex thermostability has generally proven challenging.[44]

2. RESULTS AND DISCUSSION

Phosphoramidite synthesis

5′-*O*-Dimethoxytrityl-2′-azido-2′-deoxyuridine **1**[45] was identified as a suitable substrate for CuAAC reactions. 2,2,2-Trifluoro-*N*-(prop-2-ynyl)acetamide **Av**,[46] 1-ethynylpyrene **Aw**[47] and *N*-(prop-2-ynyl)pyrene-1-carboxamide **Az**[48] were prepared as previously described, while 1-(pyren-1-yl)-prop-2-yn-1-one **Ax** and 4-(pyren-1-yl)-but-1-yne **Ay** were obtained via novel routes (Scheme 1). Thus, nucleophilic addition of MgC≡CTMS (generated in situ from trimethylsilylacetylene and MeMgBr in THF) to pyrene-1-carboxaldehyde followed by desilylation using potassium carbonate provided **Ax**′ in 58% yield. Subsequent Jones oxidation afforded **Ax** in 75% yield. Similarly, nucleophilic addition of $HC{\equiv}CCH_2ZnBr$ (generated in situ from propargyl bromide and activated zinc in THF) to pyrene-1-carboxaldehyde, followed by deoxygenation of the resultant homopropargyl alcohol using trifluoroboron etherate and triethylsilane, afforded **Ay** in 31% yield.

Room temperature CuAAC reactions between **1** and terminal alkynes **Av**-**Az** provided the corresponding triazoles **2V**-**2Z** in robust yields (60-83%), except for the click reaction involving 1-ethynylpyrene **Aw** which required heating (75 °C) to afford nucleoside **2W** in 35% yield (Scheme 2). Nucleosides **2V**-**2Z** were subsequently converted into phosphoramidites **3V**-**3Z** (51-67% yield) using 2-cyanoethyl-*N*,*N*,*N*′,*N*′-tetraisopropylphosphordiamidite (PN2-reagent) and 1*H*-tetrazole as an activator. Alternative phosphitylation conditions (e.g., PCl-reagent) were not investigated as the described route provided sufficient quantities of **3V**-**3Z** for further analysis.

ON synthesis and experimental design

Phosphoramidites **3V**-**3Z** were incorporated into ONs via machine-assisted solid-phase DNA synthesis (0.2 μmol scale) using the following non-optimized conditions (activator; coupling time; stepwise coupling yield): **3V** (4,5-dicyanoimidazole, 15min, ~80%), **3W** (5-

(ethylthio)-1*H*-tetrazole, 30min, ~90%), **3X** (5-(bis-3,5-trifluoromethylphenyl)-1*H*-tetrazole [Activator 42]; 30min, ~80%), **3Y** and **3Z** (4,5-dicyanoimidazole, 30min, ~90%). Acceptable conditions (≥80% coupling yield) were identified through progressive screening of activators (4,5-dicyanoimidazole → 5-(ethylthio)-1*H*-tetrazole → Activator 42). After workup and HPLC purification, the composition and purity of all modified ONs was verified by MALDI-MS/MS analysis (Table S1) and ion-pair reverse-phase HPLC, respectively.

The hybridization characteristics of ONs modified with **W**-**Z** monomers were examined in 13-mer sequence contexts that have previously been used to study base-discriminating fluorescent ONs.[13,15,48] Nucleotides flanking the **W**-**Z** monomers were systematically varied to explore the influence of sequence context on hybridization characteristics (Table 1). The thermostability of duplexes was evaluated by determining their thermal denaturation temperature (T_m) in a medium salt buffer ([Na^+] = 110 mM, pH 7.0). Changes in T_m-values of modified duplexes are discussed relative to T_m-values of unmodified reference duplexes (ΔT_m). The exchange of thymine (reference ONs) for uracil moieties (modified ONs) results in a decrease of 0.5 °C per incorporation,[49] but is not considered further herein.

Thermal denaturation studies

Thermal denaturation curves of DNA duplexes modified with C2′-pyrene-functionalized triazole-linked 2′-deoxyuridine monomers **W**-**Z** display similar sigmoidal monophasic transitions as unmodified reference duplexes (Fig. S1). ONs that are centrally modified with a single **W**-**Z** monomer generally display moderately decreased thermal affinity toward complementary DNA (ΔT_m for **ON5**-**ON20** between -5.0 and +1.0 °C, Table 1). Less pronounced destabilization is observed for a) ONs modified with monomer **W** where the pyrene is directly linked to the triazole moiety and, b) ONs with a central ABA-context (**ON5**/**ON9**/**ON13**/**ON17**), although the underlying mechanism is not fully understood.

Control studies using 9-mer ONs revealed that monomer **V** (i.e., without a pyrene moiety) induces larger decreases in duplex thermostability than pyrene-functionalized monomer **Z** (difference in T_m-values = 2.5-4.5 °C, Table S2). This indicates that the C2′-triazole moiety is the primary destabilizing structural feature of the **W**-**Z** monomers.

The Watson-Crick specificity of singly modified **ON5**-**ON20** was studied using DNA targets with mismatched nucleotides opposite of the modification site. Interestingly, **ON5**-**ON12** (monomers **W**/**X**) display extremely robust *universal hybridization characteristics*, i.e., mismatched duplexes exhibit minimal changes in T_m-values relative to matched duplexes (‘mismatch ΔT_m’-values between −1.5 and +2.5 °C, Table 1). ONs with a GBG-context that are hybridized to dG-mismatched targets are the exception hereto (see ‘mismatch ΔT_m’-values for **ON7** and **ON11**, Table 1). Thus, the average ‘mismatch ΔT_m’-values across the four studied sequence contexts are +0.8 °C and −0.5 °C for ONs modified with monomer **W** and **X**, respectively. In contrast, unmodified reference strands **ON1**-**ON4** display the expected mismatch discrimination profile including a) formation of substantially destabilized mismatched duplexes (average ‘mismatch ΔT_m’ = −10.0 °C, Table 1) and b) more efficient discrimination of pyrimidine-pyrimidine mismatches than of pyrimidine-purine mismatches. ONs modified with monomer **Y**, where the pyrene and triazole moieties are separated by a flexible two-carbon linker (**ON13**-**ON16**), also display universal hybridization characteristics albeit with slightly greater sequence- and mismatch-dependent variation than observed for **ON5**-**ON12** (average ‘mismatch ΔT_m’ = −1.1 °C, Table 1). ONs modified with monomer **Z**, which has the longest linker studied herein, do not display universal hybridization characteristics, although markedly reduced discrimination of mismatched targets is still observed (compare ‘mismatch ΔT_m’-values for **ON17**-**ON20** and **ON1**-**ON4**, Table 1).

We have previously studied ONs modified with C5-pyrene-functionalized triazole-linked 2′-deoxyuridine monomers in identical sequence contexts and found them to display similar 'mismatch ΔT_m'-values as ONs modified with monomer **W**/**X**/**Y**; however, significantly greater duplex destabilization was observed (average $\Delta T_m \sim -7.5$ °C).[13] In contrast, ONs modified with the related 2′-*O*-(pyren-1-yl)methyluridine or 2′-*N*-(pyren-1-ylmethyl)-2′-*N*-methylaminouridine monomers display very high thermal affinity toward complementary DNA and do not display universal hybridization characteristics.[21] These observations suggest that pyrene-functionalized triazole moieties are structural units that govern universal hybridization characteristics, and the attachment point of the pyrene-functionalized triazole moiety on the nucleotide influences duplex thermostability.

Next, **ON22**-**ON33** were prepared to study how incorporation of **W**-**Z** monomers as next-nearest neighbors influences duplex thermostability, and if the presence of **W**-**Z** monomers influences the discriminatory ability of the neighboring nucleoside for its Watson-Crick complement (Table 2).[50] Singly modified ONs with TBA- and ABT-contexts display lower thermal affinity toward complementary DNA than ONs with symmetric ABA- or TBT-contexts (e.g., compare ΔT_m-values for **ON5**, **ON8**, **ON22** and **ON23**, Table 2). This underscores the general point that new nucleotide monomers must be studied in many different sequence contexts before a full understanding of hybridization effects is reached. Incorporation of a second **X**-**Z** monomer results in approximately additive decreases in duplex thermostability, while greater-than-additive decreases are observed with monomer **W** (e.g., compare ΔT_m-values for **ON22**/**ON23**/**ON24**, Table 2).

The presence of a single **W**-**Z** monomer has, with few exceptions (**ON22**/**ON29**), only a minor effect on the discriminatory ability of neighboring base pairs (e.g., compare 'mismatch ΔT_m'-values for **ON31**/**ON32** relative to **ON21**, Table 2). This reduces the risk of undesired non-specific target binding and suggests that the pyrene-functionalized triazole units of **W**-**Z** monomers do not strongly interact with neighboring base pairs. Doubly modified ONs display poor discrimination of DNA targets with mismatched nucleotides positioned between the modification sites (e.g., compare 'mismatch ΔT_m'-values for **ON33** relative to **ON21**, Table 2), although these trends cannot be categorized as universal hybridization. We speculate that the poor mismatch specificity is caused by the dynamic local duplex structure that arises as a consequence of the low duplex thermostability.

In summary, the data demonstrate that ONs modified with C2′-pyrene-functionalized triazole-linked 2′-deoxyuridine monomers display universal hybridization characteristics with DNA targets that have mismatched nucleotides opposite of the modification site (compare 'mismatch ΔT_m'-values in Tables 1 and 2), but only limited influence on the Watson-Crick specificity of neighboring base pairs.

As a first step toward rationalizing whether intercalation of the pyrene/triazole moieties of monomers **W**-**Z** governs the observed universal hybridization characteristics, we hybridized **ON4**/**ON8**/**ON12**/**ON16**/**ON20** (TBT-context) to DNA targets containing a THF-type abasic site monomer Φ[51] opposite of monomer **W**-**Z** (for structure of monomer Φ, see Figure 1). As expected, the duplex between reference strand **ON4** and the abasic target strand is greatly destabilized relative to the matched duplex due to perturbation of the base stack (abasic ΔT_m = − 20.0 °C, Table 3). ONs modified with monomers **W**-**Z** result in the formation of remarkably thermostable duplexes with abasic target strands ('abasic ΔT_m' between −3.5 °C and +4.5 °C, Table 3). The observed trend in 'abasic ΔT_m'-values (**W**>**X**>**Y**>**Z**) demonstrates that monomers with progressively longer linkers between the pyrene and triazole moieties are less suited for stabilization of abasic sites.

Stabilization of abasic sites has been observed for monomers with extended aromatic units which a) occupy the void formed by an abasic site, and b) reestablish π- π stacking at the lesion site, and thereby partially counteracts the detrimental effects on duplex thermostability.[18,35,52–54] Full restoration of duplex thermostability, however, is rarely observed. These observations indicate that the pyrene and/or triazole moieties of monomers **W**-**Z** intercalate into the duplex core and thereby disrupt interactions between mismatched base pairs, leading to a lack of thermal preference for a particular nucleotide opposite of the modification site.

Optical spectroscopy studies

UV-Vis absorption spectra of ONs modified with monomers **W**-**Z** were recorded in absence or presence of complementary or centrally mismatched DNA targets, in order to gain additional insights into the mechanism that governs the observed universal hybridization characteristics (Figure 2); hybridization-induced intercalation of pyrene moieties is known to induce subtle bathochromic shifts.[55]

Single-stranded **ON5**-**ON8** (monomer **W**) display a single unstructured maximum in the pyrene region (λ_{max} ~ 351 nm, Figure 2), while duplexes with complementary, mismatched or abasic DNA targets display two resolved maxima at ~351 nm and ~365 nm. The lack of defined peaks for the single stranded probes (SSPs) precludes analysis of bathochromic shifts. Single-stranded **ON9**-**ON12** (monomer **X**) display two broad and virtually equally intense peaks which renders exact determination of absorption maxima unfeasible (λ_{max} ~ 385 nm and ~ 415 nm, Figure 2). Hybridization with complementary DNA results in subtle bathochromic shifts, while more pronounced shifts are observed upon hybridization with mismatched or abasic DNA. The pyrene maxima of **ON5**-**ON12** are red-shifted relative to those of unconjugated pyrenes chromophores,[13,19,21] which suggests electronic coupling between the pyrene and triazole moieties. Single-stranded **ON13**-**ON16** (monomer **Y**) and **ON17**-**ON20** (monomer **Z**), on the other hand, have structured absorption spectra with two maxima in the 'normal' region (i.e., λ_{max} ~333/348 nm and ~332/346 nm, respectively, Figure 2). Hybridization of **ON13**-**ON20** with complementary, mismatched or abasic DNA target strands results in subtle bathochromic shifts ($\Delta\lambda_{max}$ between +1 and +3 nm, Figure 2, Table S3). Thus, the absorption data are consistent with the hypothesis that the pyrene moieties of monomers **W**-**Z** intercalate into the duplex core upon hybridization with DNA targets.

Next, steady-state fluorescence emission spectra and fluorescence emission quantum yields were determined for **ON5**-**ON20** in absence or presence of complementary or centrally mismatched DNA targets (Figure 3 and Table 4).

Monomer W—Single-stranded **ON5**-**ON8** display two structured emission peaks at λ_{em} ~ 390 nm and 405 nm (Figure 3). The single-stranded probe with a central AWA-context (**ON5**) has higher fluorescence quantum yield than SSPs in other contexts (Φ_F = 0.27 vs 0.07/0.05/0.05, Table 4; see also Figure S2). This is in agreement with previous observations that adenine is the weakest quencher of pyrene fluorescence (quenching trend: G>C>T>A).[15,56,57] The spectra of the corresponding duplexes with complementary DNA have a similar shape and sequence dependency, affirming that the pyrene moiety is in close contact with the neighboring nucleobases (Figure 3, Table 4). The extensive decreases in fluorescence quantum yield (Table 4, Figure S3) upon hybridization with matched or mismatched DNA targets further corroborate this hypothesis. **ON8** (TWT-context) exhibits considerably smaller changes, presumably since the fluorophore interacts with the neighboring and only weakly quenching adenine moieties upon target binding (Figure 3, Figure S3).

Monomer X—Fluorescence emission spectra of single-stranded **ON9**-**ON12** and the corresponding duplexes with complementary or mismatched DNA targets display broad and unstructured emission peaks with maxima at λ_{em} ~ 490 nm (Figure 3). SSPs are strongly quenched with **ON11** (GXG-context) displaying the lowest intensity (Φ_F < 0.04, Table 4; Figure S2). Quantum yields are markedly increased upon hybridization of **ON9** or **ON12** with complementary/mismatched DNA targets (Table 4, Figure S3). In contrast, **ON10** or **ON11** display hybridization-induced decreases in fluorescence intensity (Table 4, Figure S3). One interpretation of these observations is that the conjugated pyrene moiety of monomer **X** intercalates into the base stack where it is quenched by neighboring cytosine and guanine moieties (**ON10**/**ON11**) but not quenched by adenine and thymine moieties (**ON9**/**ON12**). An alternative interpretation is that the pyrene moiety of monomer **X** only intercalates with **ON10**/**ON11**. However, the similar influence on duplex thermostability upon incorporation of monomer **X** irrespective of sequence context (compare ΔT_m-values for **ON9**-**ON12**, Table 1) and the hybridization-induced bathochromic shifts of pyrene absorption peaks (Figure 2) are in stronger support of the first interpretation.

Monomer Y—The fluorescence emission spectra of **ON13**-**ON16** and the corresponding duplexes with matched or mismatched DNA targets display two well-resolved pyrene peaks at λ_{em} ~380 nm and 400 nm, with an additional shoulder at λ_{em} ~ 420 nm (Figure 3). Very low quantum yields are observed (Φ_F < 0.03, Table 4), except for the single-stranded **ON13** (AYA-context). Hybridization of **ON13**-**ON16** with complementary or mismatched DNA targets generally results in decreased fluorescence intensity (Figure S3), which is consistent with an intercalating binding mode for the pyrene moiety.

Monomer Z—The fluorescence emission spectra of single-stranded **ON17**-**ON20** and the corresponding duplexes with matched or mismatched DNA targets display an unstructured peak at λ_{em} ~ 410 nm with a weaker shoulder at λ_{em} ~ 390 nm (Figure 3). The quantum yields of SSPs range from moderate to high and closely align with the previously discussed quenching trends of nucleobases (Φ_F = 0.05–0.58, Table 4; Figure S2). Hybridization with matched or mismatched DNA targets generally results in decreases (CZC/GZG-contexts) or minor increases (AZA/TZT-contexts) in quantum yields and intensity (Table 4, Figure S3), which resembles the trends with **ON9**-**ON12**.

Perhaps the most important observation toward rationalizing the universal hybridization properties of **ON5**-**ON20** is that very similar quantum yields are observed for the four duplexes between a particular probe and matched/mismatched DNA targets (e.g., compare Φ_F = 0.08/0.09/0.06/0.08 for **ON5** vs matched/mismatched DNA targets, Table 4). **ON9**, **ON12**, **ON17** and **ON20** are exceptions hereto as lower quantum yields are observed upon hybridization with dG-mismatched targets than with other DNA targets; however, this most likely reflects the fact that guanine is a strong fluorophore quencher.[56] Collectively, these observations indicate a) that the fluorophore is in a similar electronic environment within the duplex core regardless of the nucleotide opposite of the monomer, and therefore b) that the opposing nucleotide is not strongly involved in base pairing and possibly even pushed into an extrahelical position (Figure 4). Along the lines, it is interesting to note that placement of pyrene-functionalized *C*-glycosides in DNA duplexes opposite of abasic sites, which are generated via enzyme-mediated extrahelical flipping of the opposing nucleotide, is known to be stabilizing.[58–59]

Universal hybridization – RNA targets

A representative subset of modified ONs (TBT/CBT-contexts) was studied with respect to thermal denaturation, absorption and fluorescence properties with complementary/ mismatched RNA targets. Briefly described: a) incorporation of monomer **W** or **X** into ONs

results in similar decreases in thermal affinity toward complementary RNA as toward DNA, while ONs modified with monomers **Y** or **Z** are more destabilizing (Table 5; Figure S4); b) ONs modified with monomers **W** or **X** display robust universal hybridization characteristics (compare 'mismatch ΔT_m'-values for **ON6**/**ON8**/**ON12** and **ON2**/**ON4**, Table 5), while ONs modified with monomers **Y** or **Z** do not; c) pyrene absorption spectra of duplexes between modified ONs and complementary or centrally mismatched RNA targets are very similar to those of the corresponding DNA duplexes (compare Figure S5 and Figure 2); hybridization-induced bathochromic shifts with **ON14**/**ON16**/**ON18**/**ON20** (monomer **Y**/**Z**) are more subtle with RNA targets than with the corresponding DNA targets (compare Table S4 and Table S3); and d) hybridization of modified ONs to RNA targets results in very similar changes in fluorescence intensity as with DNA targets (compare Figure S6 and Figure S3).

Thus, the results indicate that the universal RNA hybridization characteristics of ONs modified with monomer **W**/**X** (**ON6**/**ON8**/**ON12**/**ON20**) also are governed by a similar mechanism as universal DNA hybridization (Figure 4).

3. CONCLUSION

Oligodeoxyribonucleotides modified with C2′-pyrene-functionalized triazole-linked 2′-deoxyuridine monomers display highly robust universal hybridization characteristics without markedly compromising duplex thermostability (Tables 1 and 5), which sets them apart from probes based on conventional universal bases such as 3-nitropyrrole or 5-nitroindole. Thermal denaturation and optical spectroscopy data suggest the universal hybridization characteristics to be a consequence of pyrene intercalation whereby the nucleotide opposite of the monomer is pushed out (Figure 4). Given the straightforward access to this monomer class via the Cu^I catalyzed [3+2] azide-alkyne cycloaddition reaction (Scheme 2), the stage is set for detailed structure-property studies for further refinement of hybridization characteristics (e.g. attachment of other aromatic moieties) and biotechnological exploration of these universal hybridization probes as degenerate PCR primers and microarray probes.

EXPERIMENTAL SECTION

General Experimental Section

Reagents and solvents were obtained from commercial vendors, of analytical grade and used without further purification. Petroleum ether of the distillation range 60–80 °C was used. Solvents were dried over activated molecular sieves: CH_2Cl_2, and *N*,*N*′-diisopropylethylamine (4Å). Water content of anhydrous solvents was verified using Karl-Fisher apparatus. Reactions were conducted under argon whenever anhydrous solvents were used. Reactions were monitored by TLC using silica gel coated plates with a fluorescence indicator (SiO_2-60, F-254) which were visualized a) under UV light and/or b) by dipping in 5% conc. H_2SO_4 in absolute ethanol (v/v) followed by heating. Silica gel column chromatography was performed with silica gel 60 (particle size 0.040–0.063 mm) using moderate pressure (pressure ball). Evaporation of solvents was carried out under reduced pressure at temperatures below 45 °C. After column chromatography, appropriate fractions were pooled, evaporated and dried at high vacuum for at least 12h to give the obtained products in high purity (>95%) as ascertained by 1D NMR techniques. Chemical shifts of ^{1}H NMR (500 MHz), ^{13}C NMR (125.6 MHz), ^{31}P NMR (121.5 MHz) and/or ^{19}F NMR (282.2 MHz) signals are reported relative to deuterated solvent or other internal standards (80% phosphoric acid for ^{31}P NMR). Exchangeable (ex) protons were detected by disappearance of ^{1}H NMR signals upon D_2O addition. Assignments of NMR spectra are based on 2D spectra (HSQC, COSY) and DEPT-spectra. Quarternary carbons are not assigned in ^{13}C NMR but verified from DEPT spectra (absence of signals). MALDIHRMS

spectra of compounds were recorded on a Q-TOF mass spectrometer using 2,5-dihydroxybenzoic acid (DHB) as a matrix and polyethylene glycol (PEG 600) as an internal calibration standard.

1-(Pyren-1-yl)-prop-2-yn-1-ol (Ax′)

Trimethylsilylacetylene (1.0 mL, 7.00 mmol) was added to MeMgBr in THF (1M, 4.0 mL, 4.00 mmol) under an argon atmosphere and stirred at rt for 1h. At this point, pyrene-1-carboxaldehyde (0.70 g, 3.00 mmol) was added and the reaction mixture was stirred at rt for another 2h. Sat. aq. NH_4Cl (~1 mL) was added and the mixture was extracted with EtOAc (2 x 20 mL). The combined organic phase was dried over Na_2SO_4 and evaporated to dryness. The resulting crude [assumed to be 1-(pyren-1-yl)-3-trimethylsilyl-prop-2-yn-1-ol] was dissolved in CH_2Cl_2 and MeOH (10 mL, 1:1, v/v) and stirred with K_2CO_3 (0.50 g, 3.62 mmol) at rt for 2h. The reaction mixture was then diluted with CH_2Cl_2 (10 mL) and successively washed with brine (20 mL) and water (20 mL). The organic phase was dried over Na_2SO_4 and evaporated to dryness. The resulting crude was purified by silica gel column chromatography (0- 50% EtOAc in petroleum ether, v/v) to afford **Ax′** (0.47 g, 58%) as a white solid material. R_f = 0.3 (25% EtOAc in petroleum ether, v/v); ESI-HRMS *m/z* 279.0783 ($[M+Na]^+$, $C_{19}H_{12}O{\cdot}Na^+$, calc 279.0780); ^{1}H NMR (DMSO-d_6) δ 8.59 (d, 1H, J = 10.0 Hz, Py), 8.35-8.29 (m, 4H, Py), 8.26 (d, 1H, J = 10.0 Hz, Py), 8.20-8.16 (m, 2H, Py), 8.09 (t, 1H, J = 7.5 Hz, Py), 6.41-6.39 (d, 1H, ex, J = 5.0 Hz, OH), 6.34-6.31 (dd, 1H, J = 5.0 Hz, 2.5 Hz, HC(OH)), 3.60 (d, 1H, J = 2.5 Hz, HC≡C); ^{13}C NMR (DMSO-d_6) δ 135.0, 130.7, 130.5, 130.1, 127.34, 127.31 (Py), 127.28 (Py), 127.25 (Py), 126.2 (Py), 125.3 (Py), 125.2 (Py), 124.65 (Py), 124.59 (Py), 124.1, 123.8, 123.7 (Py), 85.5, 76.6 (HC≡C), 60.8 (HC(OH)).

1-(Pyren-1-yl)-prop-2-yn-1-one (Ax)

The Jones reagent (2.67 M CrO_3 in 3M H_2SO_4, 1.0 mL, 2.67 mmol) was added to a solution of alcohol **Ax′** (180 mg, 0.67 mmol) in acetone (10 mL), and the reaction mixture was stirred under an ambient atmosphere at rt for 2h, whereupon it was diluted with EtOAc (20 mL), neutralized by drop-wise addition of 6M NaOH (1.0 mL) under stirring, and sequentially washed with water (30 mL) and sat. aq. $NaHCO_3$ (30 mL). The organic phase was dried over Na_2SO_4, evaporated to dryness, and the resulting crude purified by silica gel column chromatography (0–20% EtOAc in petroleum ether, v/v) to furnish **Ax** (130 mg, 75%) as a brightly yellow solid material. R_f = 0.6 (50% EtOAc in petroleum ether, v/v); ESIHRMS *m/z* 277.0626 ($[M+Na]^+$, $C_{19}H_{10}O{\cdot}Na^+$, calc 277.0624); ^{1}H NMR ($CDCl_3$) δ 9.48 (d, 1H, J = 10.0 Hz), 8.94 (d, 1H, J = 8.0 Hz), 8.28-8.23 (m, 3H), 8.19-8.14 (m, 2H), 8.07-8.02 (m, 2H), 3.53 (s, 1H); ^{13}C NMR ($CDCl_3$) δ 179.3, 135.8, 132.2 (Py), 131.31, 131.25 (Py), 131.14, 131.05 (Py), 130.6, 128.4, 127.35 (Py), 127.29 (Py), 127.1 (Py), 126.8 (Py), 124.97 (Py), 124.96, 124.95, 124.2 (Py), 124.1, 82.6, 80.1 (HC≡C). We observe distinctly different ^{1}H NMR signals in the 8.50-8.00 ppm region compared to previous reports on this compound.[60]

4-(Pyren-1-yl)-but-1-yne (Ay)

An oven-dried flask was charged with pyrene-1-carboxaldehyde (230 mg, 1.00 mmol) and activated zinc (100 mg, 1.50 mmol) and placed under an argon atmosphere. Anhydrous THF (5 mL) and propargyl bromide (0.20 mL, 1.79 mmol) were added and the reaction mixture was stirred at 45 °C for 4h. Sat. aq. NH_4Cl (1 mL) was added and the mixture was extracted with EtOAc (2 x 20 mL). The organic phase was washed with brine (20 mL) and evaporated to dryness. The resulting crude was purified by silica gel column chromatography (0–30% EtOAc in petroleum ether, v/v) to afford a crude white solid material (145 mg), which ^{1}H NMR suggested to be a ~9:1 mixture of the desired 1-(pyren-1-yl)-but-3-yn-1-ol and the corresponding allene isomer. Et_3SiH (0.20 mL, 1.25 mmol) and boron trifluoride etherate

(0.20 mL, 1.62) were added to a solution of the crude mixture in CH_2Cl_2 (5 mL), which then was stirred at rt for 1h. The reaction mixture was diluted with CH_2Cl_2 (20 mL) and sat. aq. $NaHCO_3$ (2 mL), and successively washed with brine (20 mL) and water (20 mL). The organic phase was dried over Na_2SO_4, evaporated to dryness under reduced pressure, and the resulting crude purified by silica gel column chromatography (0–3% EtOAc in petroleum ether, v/v) to afford **Ay** (80 mg, 31%) as a white solid material. R_f = 0.5 (5% EtOAc in petroleum ether, v/v); ESI-HRMS *m/z* 277.0973 ([M+Na]$^+$, $C_{20}H_{14}{\cdot}Na^+$, calc 279.0988); ^{1}H NMR ($CDCl_3$) δ 8.27-8.25 (d, 1H, *J* = 9.5 Hz, Py), 8.17-8.14 (m, 2H, Py), 8.12-8.10 (m, 2H, Py), 8.01 (ap s, 2H), 8.00-7.96 (t, 1H, *J* = 8.0 Hz, Py), 7.92-7.90 (d, 1H, *J* = 7.5 Hz, Py), 3.59 (t, 2H, *J* = 7.7 Hz, $CH_2CH_2C{\equiv}CH$), 2.72 (dt, 2H, *J* = 7.7 Hz, 2.5 Hz, $CH_2C{\equiv}CH$), 2.03 (t, 1H, *J* = 2.5 Hz, HC≡C); ^{13}C NMR ($CDCl_3$) δ 134.7, 131.6, 131.1, 130.5, 128.9, 127.8 (Py), 127.7 (Py), 127.5 (Py), 127.1 (Py), 126.1 (Py), 125.31, 125.27 (Py), 125.2, 125.1 (Py), 125.0 (Py), 123.2 (Py), 84.0, 69.6 (HC≡C), 32.8 ($CH_2CH_2C{\equiv}CH$), 21.0 ($CH_2C{\equiv}CH$).

General click reaction protocol for preparation of 2V-2Z (description for ~6 mmol scale)

5′-*O*-Dimethoxytrityl-2′-azido-2′-deoxyuridine **1**[45] and the appropriate alkyne **A** were added to a mixture of THF/*t*-BuOH/H_2O (3:1:1, v/v/v) along with sodium ascorbate and $CuSO_4{\cdot}5H_2O$ (reagent quantities, and solvent volumes are specified below). The reaction mixture was stirred under a nitrogen atmosphere until analytical TLC indicated full conversion (reaction times and temperatures specified below) whereupon it was diluted with EtOAc (10 mL). The organic phase was successively washed with sat. aq. $NaHCO_3$ (20 mL) and brine (20 mL), dried over anhydrous Na_2SO_4 and evaporated to dryness. The resulting crude was purified by silica column chromatography (eluent specified below) to afford the corresponding nucleoside **2** (yield specified below).

5′-*O*-(4,4′-Dimethoxytrityl)-2′-*C*-[4-(2,2,2-trifluoroacetamidomethyl)-*1H*-1,2,3-triazol-1-yl]-2′-deoxyuridine (2V)

Nucleoside **1** (0.40 g, 0.70 mmol), 2,2,2-trifluoro-*N*-(prop-2-ynyl)acetamide **Av**[46] (105 mg, 0.70 mmol), sodium ascorbate (70 mg, 0.35 mmol), $CuSO_4{\cdot}5H_2O$ (5 mg, 0.02 mmol) and THF/*t*-BuOH/H_2O (5 mL) were mixed, reacted (14h at rt), worked up and purified (50–100% EtOAc in petroleum ether, v/v) as described above except that the organic phase was successively washed with brine and water. Nucleoside **2V** (0.42 g, 83%) was obtained as a yellow solid material. R_f = 0.3 (80% EtOAc in petroleum ether, v/v); MALDI-HRMS *m/z* 745.2225 ([M+Na]$^+$, $C_{35}H_{34}F_3N_6O_8{\cdot}Na^+$, calc 745.2204); ^{1}H NMR (DMSO-d_6) δ 11.40 (d, 1H, ex, *J* = 2.0 Hz, H3), 10.02 (t, 1H, *J* = 6.0 Hz, $NHCOCF_3$), 8.01 (s, 1H, Tz), 7.81 (d, 1H, *J* = 8.0 Hz, H6), 7.43-7.22 (m, 9H, DMTr), 6.93-6.88 (m, 4H, DMTr), 6.42 (d, 1H, *J* = 4.5 Hz, H1′), 5.79 (d, 1H, ex, *J* = 6.0 Hz, 3′-OH), 5.50 (dd, 1H, *J* = 7.0 Hz, 4.5 Hz, H2′), 5.45 (dd, 1H, *J* = 8.0 Hz, 2.0 Hz, H5), 4.52 (m, 1H, H3′), 4.47 (d, 2H, *J* = 5.5 Hz, CH_2NHCO), 4.24-4.20 (m, 1H, H4′), 3.75 (s, 6H, CH_3O), 3.38-3.30 (m, 2H, H5′ – partial overlap with H_2O); ^{13}C NMR (DMSO-d_6) δ 162.8, 158.09, 158.08, 156.2 (q, $^{1,3}J_{CF}$ = 36 Hz, $COCF_3$), 150.1, 144.6, 142.4, 140.5 (C6), 135.3, 135.1, 129.7 (DMTr), 127.8 (DMTr), 127.7 (DMTr), 126.7 (DMTr), 124.5 (Tz), 115.8 (q, J_{CF} = 288 Hz, CF_3), 113.2 (DMTr), 101.9 (C5), 87.1 (C1′), 85.8, 83.2 (C4′), 68.8 (C3′), 64.5 (C2′), 62.8 (C5′), 55.0 (CH_3O), 34.5 (CH_2NHCO); ^{19}F-NMR (DMSO-d_6) δ -74.2.

5′-*O*-(4,4′-Dimethoxytrityl)-2′-*C*-[4-(pyrene-1-yl)-*1H*-1,2,3-triazol-1-yl]-2′-deoxyuridine (2W)

Nucleoside **1** (0.28 g, 0.49 mmol), 1-ethynylpyrene **Aw**[47] (130 mg, 0.58 mmol), sodium ascorbate (200 mg, 1.00 mmol), $CuSO_4{\cdot}5H_2O$ (25 mg, 0.10 mmol) and THF/*t*-BuOH/H_2O (10 mL) were mixed, reacted (7h at 75 °C), worked up and purified (40–70% EtOAc in petroleum ether, v/v) as described above to provide nucleoside **2W** (140 mg, 35%) as an off-white solid material. R_f = 0.5 (80% EtOAc in petroleum ether, v/v); MALDI-HRMS *m/z*

820.277 ([M+Na]$^+$, $C_{48}H_{39}N_5O_7$·Na$^+$, calc 820.274); ^{1}H NMR (DMSO-d_6) δ 11.46 (d, 1H, ex, J = 1.5 Hz, NH), 8.87 (d, 1H, J = 9.0 Hz, Py), 8.80 (s, 1H, Tz), 8.41-8.33 (m, 4H, Py), 8.27 (d, 1H, J = 9.2 Hz, Py), 8.26-8.22 (m, 2H, Py); 8.12 (t, 1H, J = 7.5 Hz, Py), 7.91 (d, 1H, J = 8.0 Hz, H6), 7.48-7.20 (m, 9H, DMTr), 6.96-6.90 (m, 4H, DMTr), 6.65 (d, 1H, J = 5.0 Hz, H1′), 5.95 (d, 1H, ex, J = 6.0 Hz, 3′-OH), 5.69 (dd, 1H, J = 7.0 Hz, 5.0 Hz, H2′), 5.54 (dd, 1H, J = 8.0 Hz, 1.5 Hz, H5), 4.69-4.64 (m, 1H, H3′), 4.40-4.36 (m, 1H, H4′), 3.76 (s, 6H, CH_3O), 3.46-3.36 (m, 2H, H5′); ^{13}C NMR (DMSO-d_6) δ 162.9, 158.2, 150.3, 145.7, 144.7, 140.8 (C6), 135.4, 135.2, 130.9, 130.6, 130.3, 129.78 (DMTr), 129.76 (DMTr), 128.0 (Py), 127.9 (DMTr), 127.73 (DMTr), 127.67 (Py), 127.5, 127.3 (Py), 127.0 (Py), 126.8 (DMTr), 126.4 (Py), 125.7 (Tz), 125.5 (Py), 125.16, 125.15 (Py), 125.09 (Py), 124.8 (Py), 124.3, 123.9, 113.3 (DMTr), 102.1 (C5), 87.4 (C1′), 85.9, 83.4 (C4′), 69.1 (C3′), 64.9 (C2′), 63.1 (C5′), 55.0 (CH_3O).

5′-*O*-(4,4′-Dimethoxytrityl)-2′-*C*-[4-(pyrene-1-ylcarbonyl)-*1H*-1,2,3-triazol-1-yl]-2′-deoxyuridine (2X)

Nucleoside **1** (0.28 g, 0.49 mmol), 1-(pyren-1-yl)-prop-2-yn-1-one **Ax** (140 mg, 0.55 mmol), sodium ascorbate (200 mg, 1.00 mmol), $CuSO_4·5H_2O$ (25 mg, 0.10 mmol) and THF/*t*-BuOH/H_2O (10 mL) were mixed, reacted (5h at rt), worked up and purified (40–90% EtOAc in petroleum ether, v/v) as described above to provide nucleoside **2X** (0.25 g, 60%) as yellow solid material. R_f = 0.4 (80% EtOAc in petroleum ether, v/v); MALDI-HRMS *m/z* 848.267 ([M+Na]$^+$, $C_{49}H_{39}N_5O_8$·Na$^+$, calc 848.270); ^{1}H NMR (DMSO-d_6) δ 11.46 (br s, 1H, ex, NH), 8.96 (s, 1H, Tz), 8.51-8.28 (m, 8H, Py), 8.17 (t, 1H, J = 7.5 Hz, Py), 7.83 (d, 1H, J = 8.0 Hz, H6), 7.44-7.21 (m, 9H, DMTr), 6.93-6.88 (m, 4H, DMTr), 6.55 (d, 1H, J = 5.0 Hz, H1′), 5.90 (d, 1H, ex, J = 5.0 Hz, 3′-OH), 5.68 (dd, 1H, J = 7.0 Hz, 5.0 Hz, H2′), 5.53 (dd, 1H, J = 8.0 Hz, 2.0 Hz, H5), 4.64-4.58 (m, 1H, H3′), 4.31-4.26 (m, 1H, H4′), 3.74 (s, 6H, CH_3O), 3.40-3.30 (m, 2H, H5′); ^{13}C NMR (DMSO-d_6) δ 188.3, 162.9, 158.1, 150.2, 147.2, 144.6, 140.8 (C6), 135.4, 135.2, 133.0, 131.8, 131.5 (Tz), 130.6, 130.0, 129.74 (DMTr), 129.72 (DMTr), 129.4 (Py), 129.1 (Py), 128.9, 127.9, 127.84 (DMTr), 127.80 (Py), 127.7 (DMTr), 127.2 (Py), 126.8 (Py), 126.7 (DMTr), 126.5 (Py), 126.1 (Py), 124.01 (Py), 123.98 (Py), 123.8, 123.5, 113.2 (DMTr), 102.0 (C5), 87.4 (C1′), 85.8, 83.3 (C4′), 69.0 (C3′), 65.0 (C2′), 63.0 (C5′), 55.0 (CH_3O).

5′-*O*-(4,4′-Dimethoxytrityl)-2′-*C*-[4-{2-(pyrene-1-yl)ethyl}-*1H*-1,2,3-triazol-1-yl]-2′-deoxyuridine (2Y)

Nucleoside **1** (0.34 g, 0.60 mmol), 4-(pyren-1-yl)-but-1-yne **Ay** (160 mg, 0.63 mmol), sodium ascorbate (0.25 g, 1.25 mmol), $CuSO_4·5H_2O$ (31 mg, 0.12 mmol) and THF/*t*-BuOH/H_2O (10 mL) were mixed, reacted (2h at rt), worked up and purified (50–100% EtOAc in petroleum ether, v/v) as described above to provide nucleoside **2Y** (0.33 g, 67%) as a white solid material. R_f = 0.3 (80% EtOAc in petroleum ether, v/v); MALDI-HRMS *m/z* 848.3046 ([M+Na]$^+$, $C_{50}H_{43}N_5O_7$·Na$^+$, calc 848.3055); ^{1}H NMR (DMSO-d_6) δ 11.44 (s, 1H, ex, NH), 8.40 (d, 1H, J = 9.0 Hz, Py), 8.30-8.19 (m, 4H, Py), 8.13 (ap s, 2H, Py), 8.06 (t, 1H, J = 8.0 Hz, Py), 8.01 (s, 1H, Tz), 7.95 (d, 1H, J = 8.0 Hz, Py), 7.82 (d, 1H, J = 8.0 Hz, H6), 7.44-7.41 (m, 2H, DMTr), 7.36-7.23 (m, 7H, DMTr), 6.94-6.90 (m, 4H, DMTr), 6.44 (d, 1H, J = 5.0 Hz, H1′), 5.79 (d, 1H, ex, J = 6.0 Hz, 3′-OH), 5.49-5.45 (m, 2H, H5, H2′), 4.54-4.49 (m, 1H, H3′), 4.27-4.22 (m, 1H, H4′), 3.75 (s, 6H, CH_3O), 3.72-3.66 (m, 2H, CH_2CH_2), 3.40-3.30 (m, 2H, H5′), 3.19-3.14 (m, 2H, CH_2CH_2); $_{13}$C NMR (DMSO-d_6) δ 162.8, 158.12, 158.11, 150.2, 145.8, 144.6, 140.5 (C6), 135.6, 135.4, 135.1, 130.8, 130.3, 129.7 (DMTr), 129.4, 128.0, 127.8 (DMTr), 127.7 (DMTr), 127.5 (Py), 127.4 (Py), 127.3 (Py), 126.7 (DMTr), 126.5 (Py), 126.1 (Py), 124.93 (Py), 124.88 (Py), 124.8 (Py), 124.2, 124.1, 123.4 (Tz), 123.2 (Py), 113.2 (DMTr), 102.0 (C5), 87.1 (C1′), 85.9, 83.3 (C4′), 68.9 (C3′), 64.3 (C2′), 62.9 (C5′), 55.0 (CH_3O), 32.6 (CH_2CH_2), 27.3 (CH_2CH_2).

5′-*O*-(4,4′-Dimethoxytrityl)-2′-*C*-[4-(pyrene-1-yl)carboxamidomethyl-*1H*-1,2,3-triazol-1-yl]-2′-deoxyuridine (2Z)

Nucleoside **1** (0.40 g, 0.70 mmol), *N*-(prop-2-ynyl)pyrene-1-carboxamide **Az**[48] (200 mg, 0.71 mmol), sodium ascorbate (50 mg, 0.25 mmol), $CuSO_4 \cdot 5H_2O$ (5 mg, 0.02 mmol) and THF/*t*-BuOH/H_2O (5 mL) were mixed, reacted (8h at rt), worked up and purified (50- 100% EtOAc in petroleum ether, v/v) as described above except that the organic phase was successively washed with brine and water. Nucleoside **2Z** (0.49 g, 83%) was obtained a yellow solid material. R_f = 0.2 (EtOAc); MALDI-HRMS *m/z* 877.2979 ($[M+Na]^+$, $C_{50}H_{42}N_6O_8 \cdot Na^+$, calc 877.2956); ^{1}H NMR (DMSO-d_6) δ 11.43 (s, 1H, ex, H3), 9.26 (t, 1H, ex, *J* = 6.0 Hz, NHCO), 8.53-8.52 (d, 1H, *J* = 9.5 Hz, Ar), 8.36-8.34 (m, 3H, Ar), 8.27-8.22 (m, 3H, Ar), 8.17-8.11 (m, 3H, Ar, Tz), 7.85 (d, 1H, *J* = 8.5 Hz, H6), 7.44-7.43 (m, 2H, DMTr), 7.35-7.24 (m, 7H, DMTr), 6.93-6.89 (m, 4H, DMTr), 6.50 (d, 1H, *J* = 4.7 Hz, H1′), 5.87 (d, 1H, ex, *J* = 5.5 Hz, 3′-OH), 5.56 (dd, 1H, *J* = 7.0 Hz, 4.7 Hz, H2′), 5.47 (d, 1H, *J* = 8.0 Hz, H5), 4.71 (d, 2H, *J* = 6.0 Hz, CH_2NHCO), 4.58-4.54 (m, 1H, H3′), 4.30-4.25 (m, 1H, H4′), 3.75 (s, 6H, CH_3O), 3.41-3.32 (m, 2H, H5′); ^{13}C NMR (DMSO-d_6) δ 168.8, 162.9, 158.13, 158.12, 150.2, 144.7, 144.6, 140.5 (C6), 135.4, 135.2, 131.6, 131.5, 130.7, 130.2, 129.8 (DMTr), 128.3 (Ar), 128.1 (Ar), 127.9 (DMTr), 127.8, 127.7 (DMTr), 127.1 (Ar), 126.8 (DMTr), 126.5 (Ar), 125.7 (Ar), 125.5 (Ar), 125.2 (Ar), 124.7 (Ar), 124.3 (Ar), 124.2 (Tz), 123.7, 123.6, 113.2 (DMTr), 102.0 (C5), 87.1 (C1′), 85.9, 83.3 (C4′), 69.0 (C3′), 64.5 (C2′), 62.9 (C5′), 55.0 (CH_3O), 35.0 (CH_2NHCO).

General phosphitylation protocol for preparation of 3V-3Z (description for ~3 mmol scale)

The appropriate nucleoside **2** was co-evaporated with anhydrous CH_2Cl_2 (5 mL) and redissolved in anhydrous CH_2Cl_2 (reagent quantities and solvent volumes are specified below). To this was added *N*,*N*-diisopropylethylamine (DIPEA), 0.45 M tetrazole in CH_3CN and 2-cyanoethyl- *N*,*N*,*N*′,*N*′-tetraisopropylphosphordiamidite (PN2-reagent). The reaction mixture was stirred at rt until analytical TLC indicated complete conversion (reaction time specified below) whereupon cold abs. EtOH (0.5 mL) was added. The reaction mixture was evaporated to dryness and the resulting residue was purified by silica gel column chromatography (eluent specified below). The crude material was triturated from cold petroleum ether to afford phosphoramidite **3** (yields specified below).

3′-*O*-(*N*,*N*-Diisopropylamino-2-cyanoethoxyphosphinyl)-5′-*O*-(4,4′-dimethoxytrityl)-2′-*C*-[4-(2,2,2-trifluoroacetamidomethyl)-*1H*-1,2,3-triazol-1-yl]-2′-deoxyuridine (3V)

Nucleoside **2V** (0.29 g, 0.40 mmol), DIPEA (0.10 mL, 0.57 mmol), tetrazole in CH_3CN (0.45 M, 1.0 mL, 0.45 mmol), PN2-reagent (0.15 mL, 0.46 mmol) and anhydrous CH_2Cl_2 (1 mL) were mixed, reacted (3h), worked up and purified (50–90% EtOAc in petroleum ether, v/v) as described above except that: a) the reaction mixture was extracted with EtOAc (5 mL) after addition of EtOH, followed by drying of the organic phase over anhydrous Na_2SO_4 and evaporation to dryness under reduced pressure and b) trituration was not performed. Phosphoramidite **3V** (0.24 g, 67%) was obtained as a white solid material. R_f = 0.3 (5% MeOH in CH_2Cl_2, v/v); MALDI-HRMS *m/z* 945.3322 ($[M+Na]^+$, $C_{44}H_{50}F_3N_8O_9 \cdot Na^+$, calc 945.3283); ^{31}P NMR ($CDCl_3$) δ 152.0, 149.8; ^{19}F NMR ($CDCl_3$) δ -75.7.

3′-*O*-(*N*,*N*-Diisopropylamino-2-cyanoethoxyphosphinyl)-5′-*O*-(4,4′-dimethoxytrityl)-2′-*C*-[4-(pyrene-1-yl)-*1H*-1,2,3-triazol-1-yl]-2′-deoxyuridine (3W)

Nucleoside **2W** (230 mg, 0.29 mmol), DIPEA (0.10 mL, 0.57 mmol), tetrazole in CH_3CN (0.45 M, 1.0 mL, 0.45 mmol), PN2-reagent (0.20 mL, 0.62 mmol) and anhydrous CH_2Cl_2 (2 mL) were mixed, reacted (4h), worked up and purified (0–4% MeOH/CH_2Cl_2, v/v) as described above to afford **3W** (180 mg, 62%) as a white powder. R_f = 0.35 (5% MeOH in

CH_2Cl_2, v/v); MALDI-HRMS *m/z* 1020.3855 ($[M+Na]^+$, $C_{57}H_{56}N_7O_8P{\cdot}Na^+$, calc 1020.3826); ^{31}P NMR ($CDCl_3$) δ 152.0, 150.5.

3′-*O*-(*N*,*N*-Diisopropylamino-2-cyanoethoxyphosphinyl)-5′-*O*-(4,4′-dimethoxytrityl)-2′-*C*-[4-(pyrene-1-ylcarbonyl)-*1H*-1,2,3-triazol-1-yl]-2′-deoxyuridine (3X)

Nucleoside **2X** (150 mg, 0.18 mmol), DIPEA (0.10 mL, 0.57 mmol), tetrazole in CH_3CN (0.45 M, 0.6 mL, 0.27 mmol), PN2-reagent (0.12 mL, 0.37 mmol) and anhydrous CH_2Cl_2 (2 mL) were mixed, reacted (3.5h), worked up and purified (0–4% MeOH/CH_2Cl_2, v/v) as described above to afford **3X** (110 mg, 59%) as a yellow solid material. R_f = 0.4 (5% MeOH in CH_2Cl_2, v/v); MALDI-HRMS *m/z* 1048.3779 ($[M+Na]^+$, $C_{58}H_{56}N_7O_9P{\cdot}Na^+$, calc 1048.3775); ^{31}P NMR ($CDCl_3$) δ 152.4, 150.9.

3′-*O*-(*N*,*N*-Diisopropylamino-2-cyanoethoxyphosphinyl)-5′-*O*-(4,4′-dimethoxytrityl)-2′-*C*-[4-{2-(pyrene-1-yl)ethyl}-*1H*-1,2,3-triazol-1-yl]-2′-deoxyuridine (3Y)

Nucleoside **2Y** (0.33 g, 0.40 mmol), DIPEA (0.10 mL, 0.57 mmol), tetrazole in CH_3CN (0.45 M, 1.5 mL), PN2-reagent (0.25 mL, 0.78 mmol) and anhydrous CH_2Cl_2 (2 mL) were mixed, reacted (3.5h), worked up and purified (0–4% MeOH/CH_2Cl_2, v/v) as described above to afford **3Y** (210 mg, 51%) as a white powder. R_f = 0.45 (5% MeOH in CH_2Cl_2, v/v); MALDI-HRMS *m/z* 1048.4147 ($[M+Na]^+$, $C_{59}H_{60}N_7O_8P{\cdot}Na^+$, calc 1048.4139); ^{31}P NMR ($CDCl_3$) δ 151.6, 150.6.

3′-*O*-(*N*,*N*-Diisopropylamino-2-cyanoethoxyphosphinyl)-5′-*O*-(4,4′-dimethoxytrityl)-2′-*C*-[4-(pyrene-1-yl)carboxamidomethyl-*1H*-1,2,3-triazol-1-yl]-2′-deoxyuridine (3Z)

Nucleoside **2Z** (0.36 g, 0.42 mmol), DIPEA (0.10 mL, 0.57 mmol), tetrazole in CH_3CN (0.45 M, 1.0 mL, 0.45 mmol), PN2-reagent (0.15 mL, 0.46 mmol) and anhydrous CH_2Cl_2 (1 mL) were mixed, reacted (3h), worked up and purified (50–90% EtOAc in petroleum ether, v/v) as described above except that: a) the reaction mixture was extracted with EtOAc (5 mL) after addition of EtOH, followed by drying of the organic phase over anhydrous Na_2SO_4 and evaporation to dryness under reduced pressure and b) trituration was not performed. Phosphoramidite **3Z** (0.28 g, 67 %) was obtained as a white solid material. R_f = 0.3 (5% MeOH in CH_2Cl_2, v/v); MALDI-HRMS *m/z* 1077.3984 ($[M+Na]^+$, $C_{59}H_{59}N_8O_9P{\cdot}Na^+$, calc 1077.4035); ^{31}P NMR ($CDCl_3$) δ 151.9, 150.1.

Synthesis and purification of ONs

Synthesis of modified oligodeoxyribonucleotides (ONs) was performed on a DNA Synthesizer using 0.2 μmol scale succinyl linked LCAA-CPG (long chain alkyl amine controlled pore glass) columns with a pore size of 500Å. Standard protocols for incorporation of DNA phosphoramidites were used. A ~50-fold molar excess of modified phosphoramidites in anhydrous acetonitrile (at 0.05 M) was used during hand-couplings using the conditions specified in the main manuscript. Moreover, extended oxidation (45s) was employed during hand-couplings. Cleavage from solid support and removal of protecting groups was accomplished upon treatment with 32% aq. ammonia (55 °C, 20 h). Purification of all modified ONs was performed by ion-pair reverse phase HPLC as described below followed by detritylation (80% aq. AcOH) and precipitation from acetone (−18 °C for 12–16h). Purification of crude ONs was performed on a HPLC system equipped with an XTerra MS C18 pre-column (10 μm, 7.8 x 10 mm) and an XTerra MS C18 column (10 μm, 7.8 x 150 mm) using a 0.05 mM TEAA (triethylammonium acetate) buffer −25% water/acetonitrile (v/v) gradient. The identity of synthesized ONs was established through MALDI-MS/MS analysis recorded in positive ions mode on a quadrupole time-of-flight tandem mass spectrometer equipped with a MALDI source using anthranilic acid as a matrix (Table S1), while purity (>80%) was verified by RP-HPLC running in analytical mode.

Thermal Denaturation Studies

Concentrations of ONs were estimated using the following extinction coefficients (OD/μmol): dG (12.01), dA (15.20), dT (8.40), dC (7.05); rG (13.70), rA (15.40), rU (10.00), rC (9.00); **V** (19.96), **W** (31.08), **X** (35.60), **Y** (27.62) and **Z** (30.95) [values for monomers **V**-**Z** were estimated through A_{260} measurements of the corresponding phosphoramidites in 1% aq. DMSO solutions]. Each strand was thoroughly mixed and denatured by heating to 80–85 °C followed by cooling to the starting temperature of the experiment. Quartz optical cells with a path length of 10 mm were used. Thermal denaturation temperatures ($T_m$values [°C]) of duplexes (1.0 μM final concentration of each strand) were measured on a UV/VIS spectrophotometer equipped with a 12-cell Peltier temperature controller and determined as the maximum of the first derivative of the thermal denaturation curve (A_{260} vs. T) recorded in medium salt buffer (T_m-buffer: 100 mM NaCl, 0.1 mM EDTA, and pH 7.0 adjusted with 10 mM Na_2HPO_4 and 5 mM Na_2HPO_4). The temperature of the denaturation experiments ranged from at least 20 °C below T_m to 20 °C above T_m. A temperature ramp of 0.5 °C/min was used in all experiments. Reported T_m-values are averages of two experiments within ± 1.0 °C.

Steady-state fluorescence emission spectra

Spectra of ONs modified with pyrenefunctionalized monomers **W**/**X**/**Y**/**Z** and the corresponding duplexes with complementary or mismatched DNA/RNA targets were recorded in non-deoxygenated thermal denaturation buffer (each strand 1.0 μM) using an excitation wavelength of λ_{ex} = 350 nm for **W**/**Y**/**Z** or λ_{ex} = 400 nm for **X**, excitation slit 5.0 nm, emission slit 5.0 nm and a scan speed of 600 nm/min. Experiments were performed at ambient temperature (~20 °C).

Determination of quantum yields

Relative fluorescence emission quantum yields (Φ_F) of modified nucleic acids (SSP or duplex) were determined using the following equation:[61] Φ_F (NA) = [Φ_F (std)/α(std)] × [IFI (NA) / A_{ex} (NA)] × [n(NA)/n(std)]^2 where Φ_F (std) is the fluorescence emission quantum yield of standard; α(std) is the slope of the integrated fluorescence intensity vs. optical intensity plot made for the standard; IFI (NA) is the integrated fluorescence intensity (λ_{em} = 360–510 nm for monomer **W**/**Y**/**Z**; λ_{em} = 425–625 nm for monomer **X**; λ_{em} = 360–600 nm for standards); A_{ex} (NA) is the optical density of the sample at the utilized excitation wavelength (λ_{ex} = 350 nm for monomer **W**/**Y**/**Z**; λ_{ex} = 400 nm for monomer **X**; λ_{ex} = 350 nm for standards; optical densities of all solutions at the excitation wavelengths were between 0.01 and 0.10); n(NA) and n(std) are refractive indexes of solvents used for sample and standard respectively (n_{water} = 1.33, $n_{ethanol}$ = 1.36, and $n_{cyclohexane}$ = 1.43). The validity of this method under our experimental set-up was ascertained by determining the quantum yield of anthracene in ethanol with respect to 9,10-diphenylanthracene in cyclohexane (Φ_F = 0.86).[61] The measured value of Φ_F = 0.28 is in excellent agreement with the reported value of (Φ_F = 0.27)[62] Subsequently, the literature value for anthracene in ethanol was used as the standard for determination of quantum yields of SSPs and duplexes.

Supplementary Material

Refer to Web version on PubMed Central for supplementary material.

Acknowledgments

We appreciate support from Award Number R01 GM088697 from the National Institute of General Medical Sciences, National Institutes of Health. We thank Dr. Lee Deobald, Prof. Andrzej J. Paszczynski (both EBI Murdock Mass Spectrometry Center, Univ. Idaho), Prof. Matthew J. Morra and Dr. Vladimir Borek (both Division of Soil & Land Resources, Univ. Idaho) for mass spectrometric analyses.

SUPPORTING INFORMATION

NMR spectra of all new compounds; MS-data of modified ONs; representative thermal denaturation profiles; T_m-values for 9-mer ONs modified with monomers **V** & **Z**; additional thermal denaturation, fluorescence and absorbance data for duplexes with matched/mismatched RNA targets. This material is available free of charge via the Internet at http://pubs.acs.org.

References

1. Rostovtsev VV, Green LG, Fokin VV, Sharpless KB. Angew Chem Int Ed. 2002; 41:2596–2599.
2. Tornøe CW, Christensen C, Meldal M. J Org Chem. 2002; 67:3057–3064. [PubMed: 11975567]
3. Amblard F, Cho JH, Schinazi RF. Chem Rev. 2009; 109:4207–4220. [PubMed: 19737023]
4. Ustinov AV, Stepanova IA, Dubnyakova VV, Zatsepin TS, Nozhevnikova EV, Korshun VA. Russ J Bioorg Chem. 2010; 36:437–481.
5. El-Sagheer AH, Brown T. Chem Soc Rev. 2010; 39:1388–1405. [PubMed: 20309492]
6. (a) Seo TS, Li Z, Ruparel H, Ju J. J Org Chem. 2003; 68:609–612. [PubMed: 12530893] (b) Gierlich J, Burley GA, Gramlich PME, Hammond DM, Carell T. Org Lett. 2006; 8:3339–3342. [PubMed: 16836400] (c) Seela F, Sirivolu VR, Chittepu P. Bioconj Chem. 2008; 19:211–224.(d) Seela F, Ming X. Helv Chim Acta. 2008; 91:1181–1200.(e) Berndl S, Herzig N, Kele P, Lachmann D, Li X, Wolfbeis OS, Wagenknecht H-A. Bioconj Chem. 2009; 20:558–564.(f) Seela F, Ingale SA. J Org Chem. 2010; 75:284–295. [PubMed: 20000692] (g) Ding P, Wunnicke D, Steinhoff H-J, Seela F. Chem Eur J. 2010; 16:14385–14396. [PubMed: 21117098] (h) Jakobsen U, Shelke SA, Vogel S, Sigurdsson ST. J Am Chem Soc. 2010; 132:10424–10428. [PubMed: 20617829] (i) Onizuka K, Shibata A, Taniguchi Y, Sasaki S. Chem Commun. 2011; 47:5004–5006.(j) Kuboyama T, Nakahara M, Yoshino M, Cui Y, Sako T, Wada Y, Imanishi T, Obika S, Watanabe Y, Suzuki M, Doi H. Bioorg Med Chem. 2011; 19:249–255. [PubMed: 21146995] (k) Mercier F, Paris J, Kaisin G, Thonon D, Flagothier J, Teller N, Lemaire C, Luxen A. Bioconj Chem. 2011; 22:108–114.
7. Burley GA, Gierlich J, Mofid MR, Nir H, Tal S, Eichen Y, Carell T. J Am Chem Soc. 2006; 128:1398–1399. [PubMed: 16448080]
8. Kumar R, El-Sagheer A, Tumpane J, Lincoln P, Wilhelmsson LM, Brown T. J Am Chem Soc. 2007; 129:6859–6864. [PubMed: 17488075]
9. Xiong H, Seela F. J Org Chem. 2011; 76:5584–5597. [PubMed: 21591729]
10. (a) Isobe H, Fujino T, Yamazaki N, Guillot-Nieckowski M, Nakamura E. Org Lett. 2008; 10:3729–3732. [PubMed: 18656947] (b) Mutisya D, Selvam C, Kennedy SD, Rozners E. Bioorg Med Chem Lett. 2011; 21:3420–3422. [PubMed: 21524577] (c) El-Sagheer AH, Brown T. Proc Natl Acad Sci USA. 2010; 107:15329–15334. [PubMed: 20713730]
11. Chittepu P, Sirivolu VR, Seela F. Bioorg Med Chem. 2008; 16:8427–8439. [PubMed: 18774721]
12. Nakahara M, Kuboyama T, Izawa A, Hari Y, Imanishi T, Obika S. Bioorg Med Chem Lett. 2009; 19:3316–3319. [PubMed: 19419865]
13. Østergaard ME, Guenther DC, Kumar P, Baral B, Deobald L, Paszczynski AJ, Sharma PK, Hrdlicka PJ. Chem Commun. 2010; 46:4929–4931.
14. Kumar TS, Wengel J, Hrdlicka PJ. ChemBioChem. 2007; 8:1122–1125. [PubMed: 17551917]
15. Østergaard ME, Kumar P, Baral B, Guenther DC, Anderson BA, Ytreberg FM, Deobald L, Paszczynski AJ, Sharma PK, Hrdlicka PJ. Chem Eur J. 2011; 17:3157–3165.
16. Østergaard ME, Hrdlicka PJ. Chem Soc Rev. 201110.1039/C1CS15014F
17. Østergaard ME, Cheguru P, Papasani MR, Hill RA, Hrdlicka PJ. J Am Chem Soc. 2010; 132:14221–14228. [PubMed: 20845923]
18. Kumar TS, Madsen AS, Østergaard ME, Wengel J, Hrdlicka PJ. J Org Chem. 2008; 73:7060–7066. [PubMed: 18710289]
19. Kumar TS, Madsen AS, Østergaard ME, Sau SP, Wengel J, Hrdlicka PJ. J Org Chem. 2009; 74:1070–1081. [PubMed: 19108636]
20. Sau SP, Kumar TS, Hrdlicka PJ. Org Biomol Chem. 2010; 8:2028–2036. [PubMed: 20401378]
21. Karmakar S, Anderson BA, Rathje RL, Andersen S, Jensen T, Nielsen P, Hrdlicka PJ. J Org Chem. 2011; 76:7119–7131. [PubMed: 21827174]

22. Yamana K, Iwase R, Furutani S, Tsuchida H, Zako H, Yamaoka T, Murakami A. Nucleic Acids Res. 1999; 27:2387–2392. [PubMed: 10325429]
23. Nakamura M, Fukunaga Y, Sasa K, Ohtoshi Y, Kanaori K, Hayashi H, Nakano H, Yamana K. Nucleic Acids Res. 2005; 33:5887–5895. [PubMed: 16237124]
24. Kalra N, Babu BR, Parmar VS, Wengel J. Org Biomol Chem. 2004; 2:2885–2887. [PubMed: 15480448]
25. Jawalekar AM, Meeuwenoord N, Cremers JSGO, Overkleeft HS, Marel GAVD, Rutjes FPJT, Delft FLV. J Org Chem. 2008; 73:287–290. [PubMed: 18052191]
26. Jørgensen AS, Shaikh KI, Enderlin G, Ivarsen E, Kumar S, Nielsen P. Org Biomol Chem. 2011; 9:1381–1388. [PubMed: 21210043]
27. Kiviniemi A, Virta P, Drenichev MS, Mikhailov SN, Lönnberg H. Bioconj Chem. 2011; 22:1249–1255.
28. Patil RV, Dekker EE. Nucleic Acids Res. 1990; 18:3080–3080. [PubMed: 2190190]
29. Nichols R, Andrews PC, Zhang P, Bergstrom DE. Nature. 1994; 369:492–493. [PubMed: 8202140]
30. Loakes D, Brown DM, Linde S, Hill F. Nucleic Acids Res. 1995; 23:2361–2366. [PubMed: 7630712]
31. Chizhikov V, Wagner M, Ivshina A, Hoshino Y, Kapikian AZ, Chumakov K. J Clin Microbiol. 2002; 40:2398–2407. [PubMed: 12089254]
32. Too, K.; Loakes, D. Universal Base Analogues and their Application to Biotechnology. In: Herdewijn, P., editor. Modified Nucleosides: In Biochemistry, Biotechnology and Medicine. WILEY-VCH; Weinheim: 2008. p. 277-303.
33. Loakes D, Brown DM. Nucleic Acids Res. 1994; 22:4039–4043. [PubMed: 7937128]
34. Berger M, Wu Y, Ogawa AK, McMinn DL, Schultz PG, Romesberg FE. Nucleic Acids Res. 2000; 28:2911–2914. [PubMed: 10908353]
35. Matray TJ, Kool ET. J Am Chem Soc. 1998; 120:6191–6192. [PubMed: 20852721]
36. Babu BR, Wengel J. Chem Commun. 2001:2114–2115.
37. Raunak, Babu BR, Parmar VS, Harrit NH, Wengel J. Org Biomol Chem. 2004; 2:80–89. [PubMed: 14737663]
38. MacKinnon KF, Qualley DF, Woski SA. Tetrahedron Lett. 2007; 48:8074–8077.
39. Seela F, Chen Y. Nucleic Acids Res. 1995; 23:2499–2505. [PubMed: 7630728]
40. Acedo M, De Clercq E, Eritja R. J Org Chem. 1995; 60:6262–6269.
41. Cubero E, Güimil-García R, Luque FJ, Eritja R, Orozco M. Nucleic Acids Res. 2001; 29:2522–2534. [PubMed: 11410660]
42. Seela F, Debelak H. Nucleic Acids Res. 2000; 28:3224–3232. [PubMed: 10954589]
43. Koller AN, Bozilovic J, Engels JW, Gohlke H. Nucleic Acids Res. 2010; 38:3133–3146. [PubMed: 20081201]
44. For a successful example, see Köhler O, Jarikote DV, Seitz O. ChemBioChem. 2005; 6:69–77. [PubMed: 15584015]
45. Patra A, Richert C. J Am Chem Soc. 2009; 131:12671–12681. [PubMed: 19722718]
46. Trybulski EJ, Zhang J, Kramss RH, Mangano RM. J Med Chem. 1993; 36:3533–3541. [PubMed: 8246221]
47. Liu F, Tang C, Chen QQ, Li SZ, Wu HB, Xie LH, Peng B, Wei W, Cao Y, Huang W. Org Electron. 2009; 10:256–265.
48. Okamoto A, Kanatani K, Saito I. J Am Chem Soc. 2004; 126:4820–4827. [PubMed: 15080686]
49. Sanghvi YS, Hoke GD, Freier SM, Zounes MC, Gonzalez C, Cummins L, Sasmor H, Cook PD. Nucleic Acids Res. 1993; 21:3197–3203. [PubMed: 8393563]
50. Oliver JS, Parker KA, Suggs JW. Org Lett. 2001; 3:1977–1980. [PubMed: 11418028]
51. Millican TA, Mock GA, Chauncey MA, Patel TP, Eaton MAW, Gunning J, Cutbush SD, Neidle S, Mann J. Nucleic Acids Res. 1984; 12:7435–7453. [PubMed: 6548562]
52. Langenegger SM, Häner R. ChemBioChem. 2005; 6:848–851. [PubMed: 15776408]

53. Nakano S, Uotani Y, Uenishi K, Fujii M, Sugimoto N. Nucleic Acids Res. 2005; 33:7111–7119. [PubMed: 16361269]
54. Verhagen C, Bryld T, Raunkjær M, Vogel S, Buchalová K, Wengel J. Eur J Org Chem. 2006:2538–2548.
55. Dougherty G, Pilbrow JR. Int J Biochem. 1984; 16:1179–1192. [PubMed: 6397369]
56. Manoharan M, Tivel KL, Zhao M, Nafisi K, Netzel TL. J Phys Chem. 1995; 99:17461–1747.
57. Seo YJ, Ryu JH, Kim BH. Org Lett. 2005; 7:4931–4933. [PubMed: 16235925]
58. Jiang YL, Kwon K, Stivers JT. J Biol Chem. 2001; 276:42347–42354. [PubMed: 11551943]
59. Beuck C, Singh I, Bhattacharya A, Hecker W, Parmar VS, Seitz O, Weinhold E. Angew Chem Int Ed. 2003; 42:3958–3960.
60. Fleming DA, Thode CJ, Williams ME. Chem Mater. 2006; 18:2327–2334.
61. Morris JV, Mahaney MA, Huber JR. J Phys Chem. 1976; 80:969–974.
62. Melhuish WH. J Phys Chem. 1961; 65:229–235.

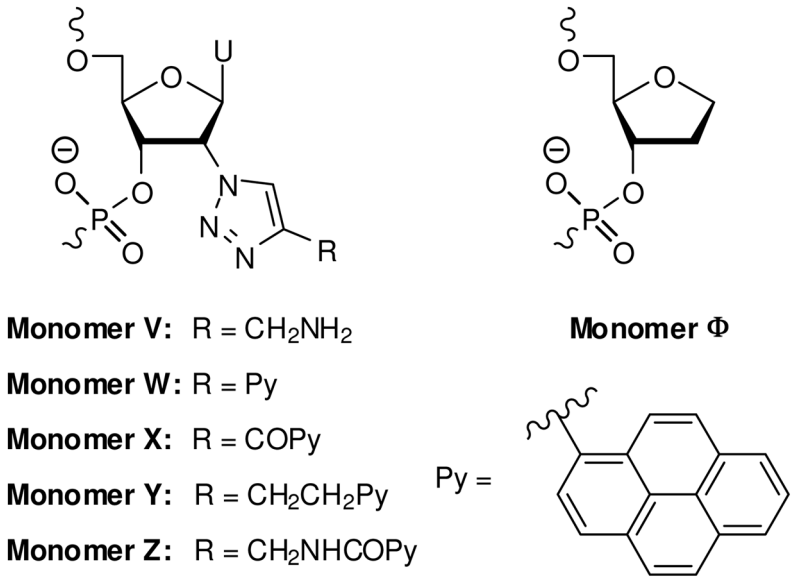

Figure 1.
Structures of C2′-pyrene-functionalized triazole-linked 2′-deoxyuridine monomers and other monomers studied herein.

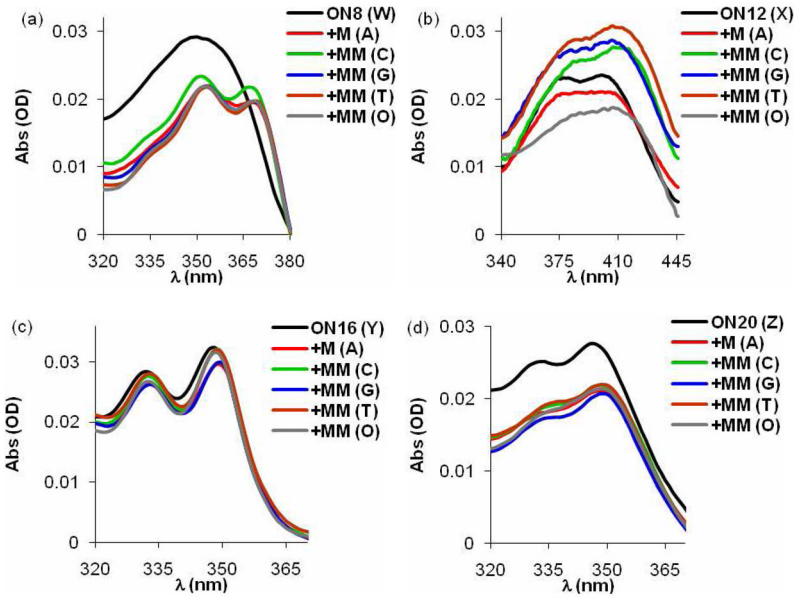

Figure 2.

Representative absorption spectra of single-stranded **ON8**/**ON12**/**ON16**/**ON20** (a–d) and their duplexes with matched (M) and centrally mismatched (MM) DNA targets: 3′-GCGTT A**B**A TTGCG. Nucleotide opposite of modification is mentioned in parenthesis. Spectra were recorded in thermal denaturation buffer at T = 20 °C using 1.0 μM concentration of each strand. Note that different X-axes are used. “O” denotes THF-type abasic site monomer Φ(Figure 1).

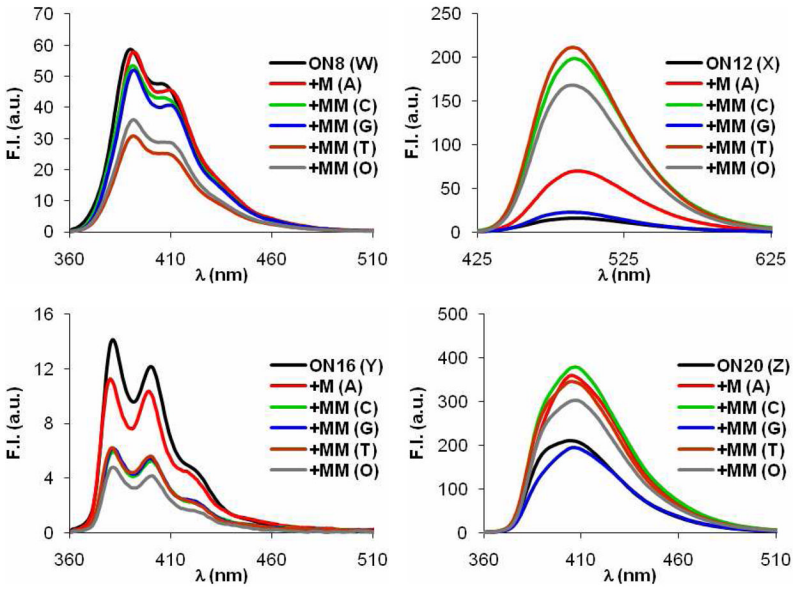

Figure 3.

Steady-state fluorescence emission spectra of single-stranded **ON8**/**ON12**/**ON16**/**ON20** (TTT-context) and duplexes with matched (M) or centrally mismatched (MM) DNA. Recorded in thermal denaturation buffer at T = 20 °C using 1.0 μM of each strand and λ_{ex} = 350 nm (monomers **W**, **Y** and **Z**) or λ_{ex} = 400 nm (monomer **X**). DNA targets 3′-GCGTT A**B**A TTGCG. Nucleotide opposite of modification is mentioned in parenthesis. Note that different axes are used. “O” denotes THF-type abasic site monomer Φ (Figure 1).

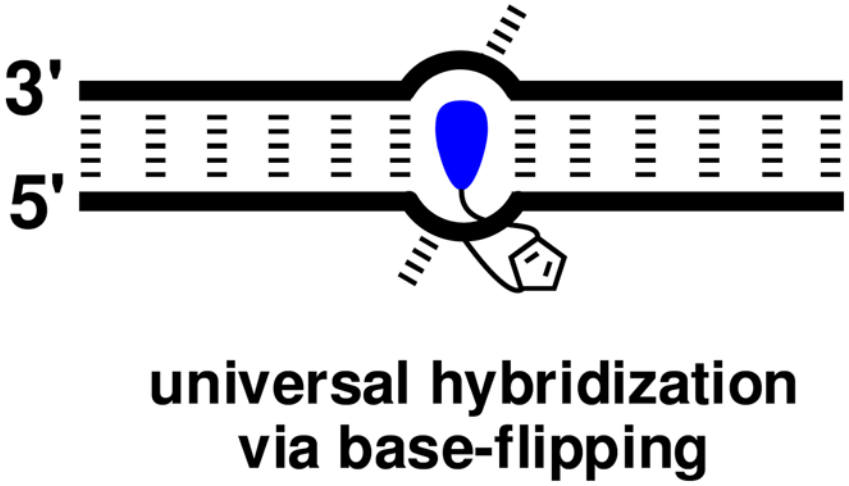

Figure 4.
Illustration of putative mechanism resulting in universal hybridization.

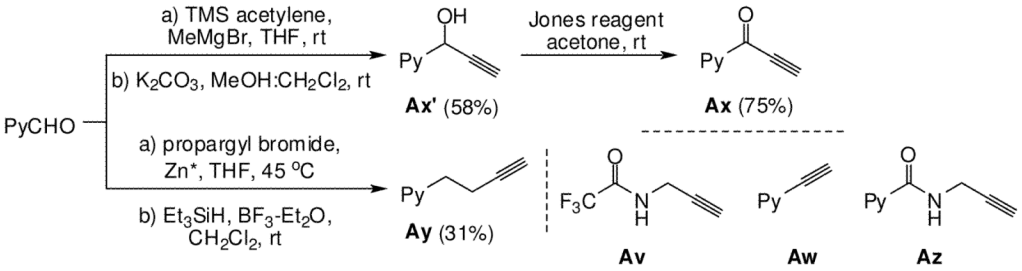

Scheme 1.
Synthesis and structures of terminal alkynes.

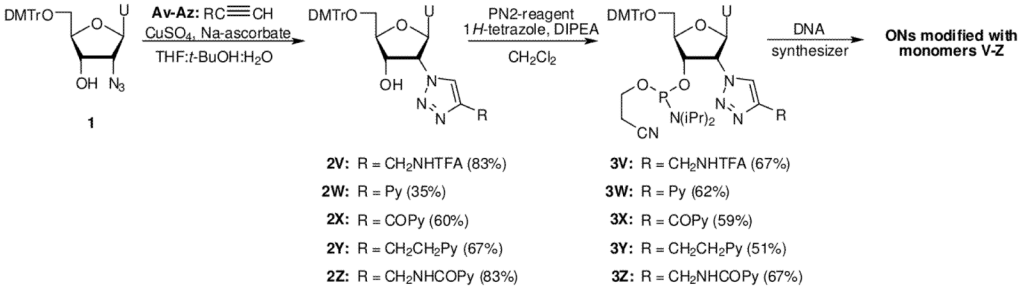

Scheme 2.
Synthesis of C2′-pyrene-functionalized triazole-linked uridine phosphoramidites **3V**-**3Z**.

Table 1

T_m-values of duplexes between centrally modified ONs and complementary or centrally mismatched DNA targets.[a]

ON	Sequence	T_m (ΔT_m) [°C] B =A	Mismatch ΔT_m [°C] C	G	T	Avg. mismatch ΔT_m seq. [°C]	Avg. mismatch ΔT_m series [°C]
1	5′-CGCAA A**T**A AACGC	48.5	−10.0	−5.0	−9.0	−8.0 ± 2.6	−10.0 ± 2.2
2	5′-CGCAA C**T**C AACGC	55.5	−13.5	−9.5	−9.0	−10.7 ± 2.5	
3	5′-CGCAA G**T**G AACGC	55.5	−13.0	−9.5	−10.0	−10.8 ± 1.9	
4	5′-CGCAA T**T**T AACGC	48.5	−11.0	−9.0	−11.0	−10.3 ± 1.2	
5	5′-CGCAA A**W**A AACGC	48.0 (−0.5)	+1.0	+1.5	+1.5	+1.3 ± 0.3	+0.8 ± 1.9
6	5′-CGCAA C**W**C AACGC	53.5 (−2.0)	+0.5	+2.0	+2.5	+1.7 ± 1.0	
7	5′-CGCAA G**W**G AACGC	51.5 (−4.0)	+1.0	−4.5	0.0	−1.2 ± 2.9	
8	5′-CGCAA T**W**T AACGC	47.0 (−1.5)	+2.5	−0.5	+2.0	+1.3 ± 1.6	
9	5′-CGCAA A**X**A AACGC	46.5 (−2.0)	+1.0	+0.5	+1.0	+0.8 ± 0.3	−0.5 ± 2.2 1
10	5′-CGCAA C**X**C AACGC	52.0 (−3.5)	−1.5	0.0	−0.5	−0.7 ± 0.8	
11	5′-CGCAA G**X**G AACGC	52.5 (−3.0)	+0.5	−7.0	−0.5	−2.3 ± 4.1	
12	5′-CGCAA T**X**T AACGC	44.5 (−4.0)	+1.0	−1.0	0.0	0.0 ± 1.0	
13	5′-CGCAA A**Y**A AACGC	49.5 (+1.0)	+1.5	0.0	+1.0	+0.8 ± 0.8	−1.1 ± 2.1
14	5′-CGCAA C**Y**C AACGC	50.5 (−5.0)	−5.0	−1.0	−2.5	−2.8 ± 2.0	
15	5′-CGCAA G**Y**G AACGC	53.0 (−2.5)	+1.5	−3.5	+0.5	−0.5 ± 2.6	
16	5′-CGCAA T**Y**T AACGC	44.5 (−4.0)	−2.0	−2.0	−1.5	−1.8 ± 0.3	
17	5′-CGCAA A**Z**A AACGC	47.0 (−1.5)	−5.5	−2.5	−4.0	−4.0 ± 1.5	−4.1 ± 1.6
18	5′-CGCAA C**Z**C AACGC	51.5 (−4.0)	−6.5	−1.0	−4.0	−3.8 ± 2.8	
19	5′-CGCAA G**Z**G AACGC	52.0 (−3.5)	−2.0	−6.0	−4.0	−4.0 ± 2.0	
20	5′-CGCAA T**Z**T AACGC	45.5 (−3.0)	−4.5	−5.0	−4.0	−4.5 ± 0.5	

[a] T_m-values determined as maximum of the first derivative of denaturation curves (A_{260} vs T) recorded in thermal denaturation buffer ([Na^+] = 110 mM, [Cl^-] = 100 mM, pH 7.0 (NaH_2PO_4/Na_2HPO_4)) using 1.0 μM of each strand. T_m-values are averages of at least two measurements within 1.0 °C. "ΔT_m" = change in T_m relative to unmodified reference duplex. "Mismatch ΔT_m" = change in T_m relative to fully matched duplex (B = A). "Avg Mismatch ΔT_m seq" = average of all three "Mismatch ΔT_m"-values for a given probe. "Avg Mismatch ΔT_m series" = average of all twelve "Mismatch ΔT_m"-values of all four studied sequences within a monomer series. "±" denotes standard deviation. DNA targets: 3′-GCGTT T**B**T TTGCG (for **ON1**/**ON5**/**ON9**/**ON13**/**ON17**), 3′-GCGTT G**B**G TTGCG (for **ON2**/**ON6**/**ON10**/**ON14**/**ON18**), 3′-GCGTT C**B**C TTGCG (for **ON3**/**ON7**/**ON11**/**ON15**/**ON19**) and 3′-GCGTT A**B**A TTGCG (for **ON4**/**ON8**/**ON12**/**ON16**/**ON20**). For structures of monomers **W**-**Z** see Figure 1.

Table 2

T_m-values of duplexes between **ON21-ON33** and complementary or centrally mismatched DNA targets.[a]

		DNA: 5′-CGCAA ABA AACGC			
		T_m (ΔT_m) [°C]	Mismatch ΔT_m [°C]		
ON	Sequence	B=T	A	C	G
21	3′-GCGTT TAT TTGCG	48.5	−10.0	−10.0	−5.5
22	3′-GCGTT TA**W** TTGCG	46.5 (−2.0)	−17.0	−9.0	−12.0
23	3′-GCGTT **W**AT TTGCG	41.0 (−7.5)	−11.5	−10.0	−5.5
24	3′-GCGTT **W**A**W** TTGCG	35.0 (−13.5)	nt	−3.5	nt
25	3′-GCGTT TA**X** TTGCG	44.0 (−4.5)	−9.0	−7.5	−5.0
26	3′-GCGTT **X**AT TTGCG	42.0 (−6.5)	−10.5	−11.5	−6.0
27	3′-GCGTT **X**A**X** TTGCG	36.5 (−12.0)	−2.5	−4.5	+0.5
28	3′-GCGTT TA**Y** TTGCG	40.0 (−8.5)	−7.0	−7.0	−5.0
29	3′-GCGTT **Y**AT TTGCG	42.5 (−6.0)	−6.0	−2.5	−7.0
30	3′-GCGTT **Y**A**Y** TTGCG	34.5 (−14.0)	−4.5	−3.5	−4.5
31	3′-GCGTT TA**Z** TTGCG	42.5 (−6.0)	−7.0	−8.5	−7.5
32	3′-GCGTT **Z**AT TTGCG	44.0 (−4.5)	−11.5	−12.0	−9.0
33	3′-GCGTT **Z**A**Z** TTGCG	39.5 (−9.0)	−2.5	−0.5	−3.5

[a]Conditions and definitions as described in footnote of Table 1. “nt” = no transition.

Table 3

T_m-values of duplexes between centrally modified ONs (TBT-context) and complementary DNA or targets containing a central abasic site.[a]

ON	Sequence	3′-GCGTT ATA TTGCG T_m [°C]	3′-GCGTT AΦA TTGCG Abasic ΔT_m [°C]
4	5′-CGCAA T**T**T AACGC	48.5	−20.0
8	5′-CGCAA T**W**T AACGC	47.0	+4.5
12	5′-CGCAA T**X**T AACGC	44.5	+2.0
16	5′-CGCAA T**Y**T AACGC	44.5	+0.5
20	5′-CGCAA T**Z**T AACGC	45.5	−3.5

[a]Conditions as described in footnote of Table 1. "Abasic ΔT_m" = change in T_m relative to fully matched duplex. Φ = abasic monomer (for structure, see Figure 1).

Table 4

Relative fluorescence emission quantum yield (Φ_F) of **ON5-ON20** in the absence (SSP) or presence of matched (M) or centrally mismatched (MM) DNA targets.[a]

		Φ_F				
ON	**Sequence**	**SSP**	**+M (A)**	**+MM (C)**	**+MM (G)**	**+MM (T)**
5	5′-CGCAA A**W**A AACGC	0.27	0.08	0.09	0.06	0.08
6	5′-CGCAA C**W**C AACGC	0.07	0.02	0.02	0.02	0.01
7	5′-CGCAA G**W**G AACGC	0.05	0.03	0.01	0.02	0.01
8	5′-CGCAA T**W**T AACGC	0.05	0.07	0.06	0.06	0.04
9	5′-CGCAA A**X**A AACGC	0.02	0.25	0.33	0.10	0.25
10	5′-CGCAA C**X**C AACGC	0.02	<0.01	<0.01	<0.01	<0.01
11	5′-CGCAA G**X**G AACGC	<0.01	<0.01	<0.01	<0.01	<0.01
12	5′-CGCAA T**X**T AACGC	0.04	0.16	0.35	0.04	0.32
13	5′-CGCAA A**Y**A AACGC	0.09	0.02	0.02	0.02	0.03
14	5′-CGCAA C**Y**C AACGC	0.01	0.02	<0.01	<0.01	<0.01
15	5′-CGCAA G**Y**G AACGC	0.03	0.01	0.01	0.01	<0.01
16	5′-CGCAA T**Y**T AACGC	0.01	<0.01	<0.01	<0.01	<0.01
17	5′-CGCAA A**Z**A AACGC	0.58	0.52	0.78	0.29	0.79
18	5′-CGCAA C**Z**C AACGC	0.24	0.15	0.17	0.15	0.19
19	5′-CGCAA G**Z**G AACGC	0.05	0.04	0.02	0.02	0.03
20	5′-CGCAA T**Z**T AACGC	0.27	0.57	0.58	0.31	0.52

[a] Relative to quantum yield of anthracene in ethanol (0.27). Recorded in thermal denaturation buffer at T = 20 °C using 1.0 μM concentration of each strand and λ_{ex} = 350 nm and λ_{em} = 360–510 nm (monomers **W**, **Y** and **Z**) or λ_{ex} = 400 nm and λ_{em} = 425–625 nm (monomer **X**). For DNA targets, see footnote Table 1. Nucleotide opposite of modification is mentioned in parenthesis.

Table 5

T_m-values of duplexes between centrally modified ONs and complementary or centrally mismatched RNA targets.[a]

		T_m (ΔT_m) [°C]	Mismatch ΔT_m [°C]		
ON	**Sequence**	**B= A**	**C**	**G**	**U**
2	5′-CGCAA C**T**C AACGC	51.5	−15.5	−3.0	−13.5
4	5′-CGCAA T**T**T AACGC	40.5	−19.0	−3.5	−17.0
6	5′-CGCAA C**W**C AACGC	47.0 (−4.5)	+1.0	+0.0	+0.5
8	5′-CGCAA T**W**T AACGC	42.0 (+1.5)	+3.0	+0.5	+1.5
12	5′-CGCAA T**X**T AACGC	38.0 (−2.5)	+1.0	+0.0	+1.0
14	5′-CGCAA C**Y**C AACGC	43.5 (−8.0)	−2.0	−5.0	−4.0
16	5′-CGCAA T**Y**T AACGC	36.0 (−4.5)	+1.5	−1.0	−1.0
18	5′-CGCAA C**Z**C AACGC	44.5 (−7.0)	−3.0	−8.0	−7.0
20	5′-CGCAA T**Z**T AACGC	36.5 (−4.0)	−12.0	−7.5	−13.0

[a] Conditions and definitions as described in footnote of Table 1. RNA targets: 3′-GCGUU G**BG** UUGCG (for **ON2/ON6/ON14/ON18**) and 3′-GCGUU A**B**A UUGCG (for **ON4/ON8/ON12/ON16/ON20**).